

Motion of the Ugamak Slide, probable source of the tsunami of 1 April 1946

Gerard J. Fryer¹ and Philip Watts²

¹*Hawaii Institute of Geophysics and Planetology, University of Hawaii at Manoa, Honolulu, Hawaii, U.S.A.*

²*Applied Fluids Engineering, Inc., Long Beach, California, U.S.A.*

Abstract. The eastern Aleutian tsunami of 1 April 1946 exhibited large waves and caused extensive damage throughout the eastern Pacific, yet the source region inferred from aftershocks was only 80 km wide. Near-source run-ups showed a rapid variation with distance, consistent with a small source. Reconciling the near-source variation with the transpacific reach of the tsunami seems impossible for any sensible earthquake source. We have earlier argued that a landslide source fits the combined near-field and far-field observations better than an earthquake. Here we show that the motion of the landslide was fast enough to couple efficiently with the tsunami to produce large waves in the far field. Perfect coupling, however, was never accomplished because the slide motion was always less than celerity. Waves in the reverse direction to slide motion were therefore not suppressed, resulting in 35 m run-up at Scotch Cap on Unimak Island. We further show that the arrival time of the tsunami at Scotch Cap demands a landslide at the edge of the Aleutian Shelf at precisely the location of the 1200 km² Ugamak Slide.

1. Introduction

The tsunami of 1 April 1946, from Unimak Island in the eastern Aleutians, remains enigmatic. Large run-ups throughout the eastern Pacific (Fig. 1) suggest an extended seismic source, but the aftershock zone was only 80 km wide (Sykes, 1971). Near-source run-ups varied from 35 m at Scotch Cap to 6 m at Sanak Village only 120 km away (Lander, 1996). Such rapid variation would be expected from a shallow earthquake with rupture less than 100 km wide, but no such small-aperture source can produce the narrow beam of large waves observed in the far field.

In an earlier paper (Fryer *et al.*, 2001), we proposed that the source of the tsunami was not a tectonic earthquake but a landslide, a collapse feature visible in GLORIA sidescan sonar images collected by the U.S. Geological Survey (Karl and Carlson, 1996). We call the feature the Ugamak Slide. It descends from the shelf edge at 105 m to at least 4000 m depth (Fig. 2), and has an area of 1200 km². To explain the large wave heights and narrow beam of the tsunami in the far field, we hypothesized that for much of its motion the Ugamak Slide was traveling at or near the local celerity (the phase velocity of a tsunami in water of that depth), resulting in efficient coupling between slide and tsunami (Fryer *et al.*, 2001). This would produce large waves in the direction of slide motion, but with rapid fall off with azimuth, qualitatively matching the observations of Fig. 1.

Our near-celerity hypothesis needs modification. The gentle slope of

¹University of Hawaii at Manoa, Hawaii Institute of Geophysics and Planetology, 1680 East-West Road, POST 602, Honolulu, HI 96822, U.S.A. (gerard@hawaii.edu)

²Applied Fluids Engineering, Inc., 5710 East 7th Street, PMB #237, Long Beach, CA 90803, U.S.A. (phil.watts@appliedfluids.com)

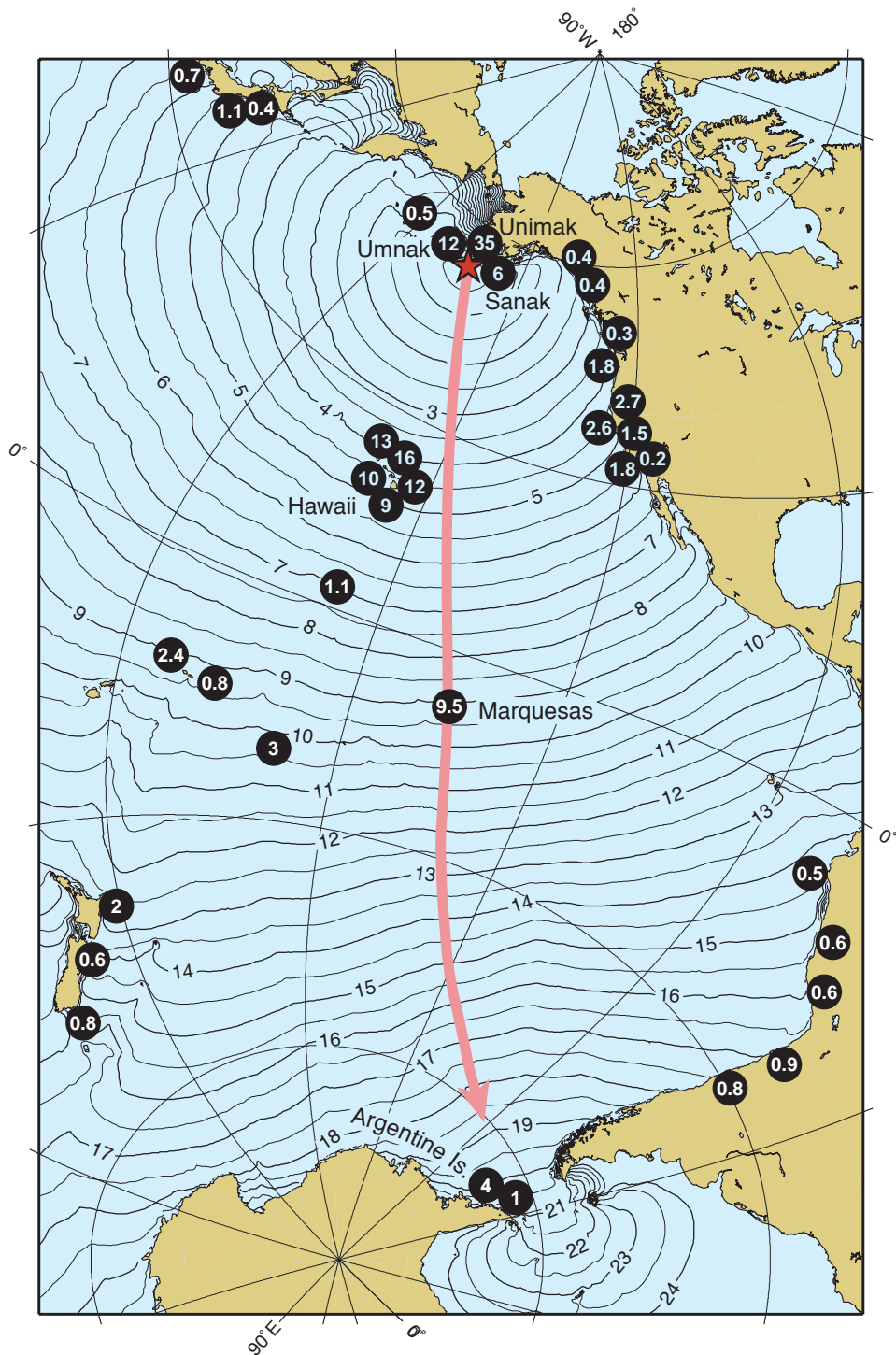


Figure 1: Travel times and run-ups for the Unimak tsunami. The arrow is the trench-normal ray from Unimak Island. Circled numbers are run-ups in meters. Run-ups larger than 3 m only occurred close to the central ray.

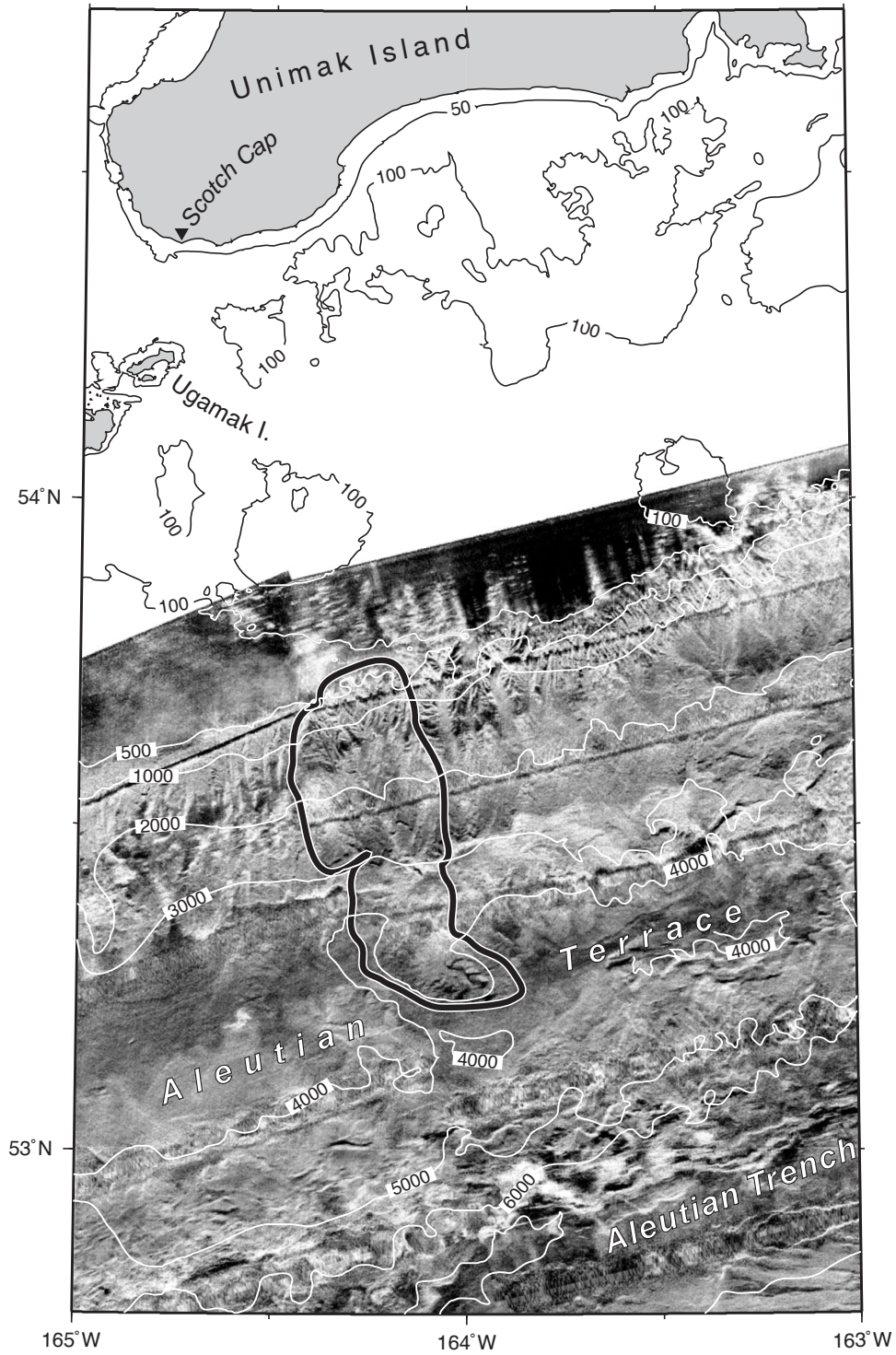


Figure 2: Setting of the Ugamak Slide. The main part of the slide is outlined in black. Contours are depths in meters. The USGS GLORIA sidescan image exists only for deep water. In the sidescan image white denotes a strong backscattered return and black a weak return.

the Aleutian forearc means acceleration too low for a landslide to catch up with the tsunami it is generating, so celerity could never be reached. Further, a slide traveling near celerity could not explain the near-field wave heights. The 1-D analyses of Tinti and Bortolucci (2000) show that as a slide approaches celerity, the forward-traveling waves (those moving in the direction of slide motion) grow at the expense of the backward-traveling waves until, at celerity, the backward traveling waves vanish (they reappear if the slide accelerates through celerity). The waves advancing into the Pacific in 1946 were large, but the waves traveling in the reverse direction had to be of comparable size to produce the 35 m run-up at Scotch Cap. If the Ugamak Slide was indeed the source of the tsunami of 1946, then it had to move at an appreciable fraction of celerity for much of its motion to produce large waves on a transpacific beam, but not move so fast as to suppress the waves attacking Scotch Cap. The motion of the slide and its generation of the tsunami is the main subject of this paper.

One other area was inadequately treated in our earlier paper: the location of the slide. We claimed that the Ugamak Slide satisfied perfectly the observed travel time to Scotch Cap (Fryer *et al.*, 2001), but provided no justification for that claim. We correct that omission here.

2. Location of the Landslide Source

We assume that an earthquake produced shaking severe enough and sustained enough to drive poorly drained sediments of the forearc to failure, so creating the Ugamak Slide. Failure occurred either during the earthquake or within a few minutes of it. Severe shaking for 30–40 s was experienced by personnel at Scotch Cap (Lander, 1996), while body-wave data indicates a source duration in excess of 100 s (Pelayo, 1990). The shaking might have been the earthquake, or the landslide, or some combination. A landslide contribution to the drawn-out source duration is perhaps a more prosaic explanation than the exceptionally slow earthquake rupture proposed by Pelayo and Wiens (1992).

The tsunami reached Scotch Cap 48 min after the earthquake (Lander, 1996). This travel time is from entries in the log of the U.S. Coast Guard Station at Scotch Cap, a direction-finding station and lighthouse (the tsunami destroyed the lighthouse and severely damaged the station; there were five deaths). The log lists the earthquake, a major aftershock, and the tsunami, at “about 0130,” 0157, and 0218, respectively, all local time. Times from the log, as well as elapsed times deduced from log entries, should be correct to within 2 min (the actual times of the earthquakes were 0128:56 and 0155:47).

Travel times to Scotch Cap are shown in Fig. 3. Two prospective tsunami sources, the Ugamak Slide and the best-fitting earthquake (Pelayo, 1990; Johnson and Satake, 1997), are also shown. The travel time range from 46 to 50 min is tinted red; the range from 38.5 to 42.5 min is tinted orange.

A shallow subduction earthquake produces uplift over the shallow (seaward) part of the rupture, with subsidence to landward. For a tsunami

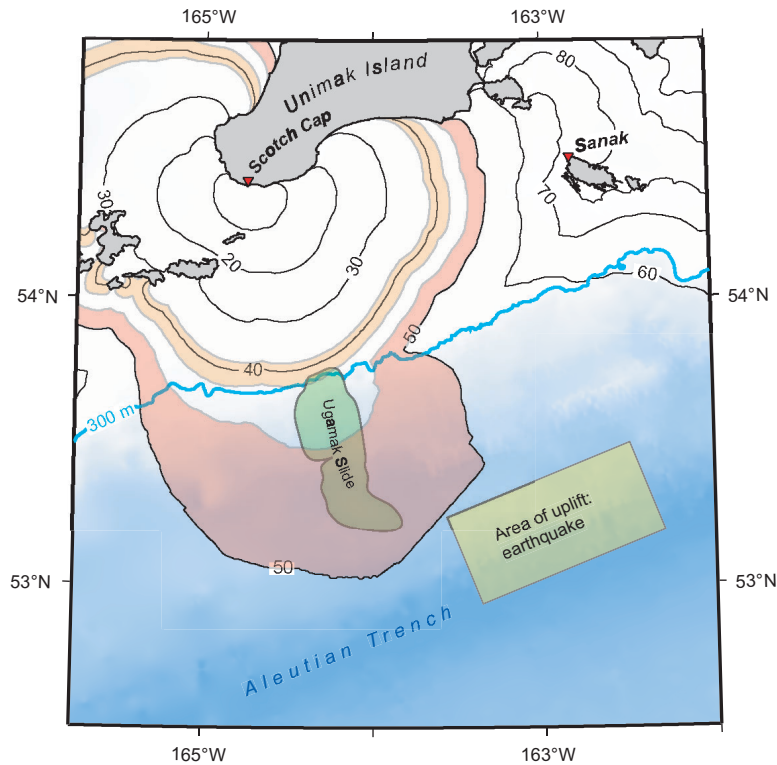


Figure 3: Tsunami travel times to Scotch Cap. Contours are in minutes. The 46–50-min zone is tinted red, the 38.5–42.5-min zone is tinted orange. The Ugamak Slide and the uplifted region of the best-fitting earthquake source are outlined. Water depths are denoted by the blue tint; the 300 m depth contour is just downslope from the shelf edge.

generated directly by an earthquake, the arrival time of the first positive wave on the adjacent coast is well approximated by assuming that the positive wave above the uplift moves shoreward at the celerity (Geist, 1998, Fig. 3). For an earthquake-generated tsunami to satisfy the 48 ± 2 min travel time to Scotch Cap, the area of uplift of the earthquake would have to fall within the red-tinted 46–50-min zone of Fig. 3. It does not. The earthquake source is in error. We cannot, however, dismiss an earthquake origin outright. The location of the 1946 earthquake and its aftershocks are only poorly constrained (Pelayo, 1990); it might be possible to nudge the rupture zone far enough southwest to intersect the 46–50-min zone.

A landslide source is more closely constrained by travel times. A submarine landslide draws down the sea surface above the head of the slide and pushes up the sea surface over a broad area seaward of the advancing toe. Most of the energy of the resulting tsunami is carried in three waves which each expand cylindrically: the positive wave ahead of the slide, the negative wave above the slide, and the positive wave from the first oscillation of the drawdown (Heinrich *et al.*, 2000). In the direction opposite to slide motion, the first positive wave is the sum of the first positive oscillation and the reverse-traveling positive wave from ahead of the slide. This composite wave

can be thought of as originating above the head of the slide at a time of one half the predominant period of the tsunami.

In 1946 the predominant period recorded on tide gauges in Hawaii and California (Iida *et al.*, 1967; Lander and Lockridge, 1989), was 15 min. To satisfy the 48 ± 2 min travel time to Scotch Cap, a landslide source for the tsunami would thus have to have its headwall somewhere within the orange-tinted 38.5–42.5-min zone of Fig. 3.

The Aleutian Shelf edge, marked by the 300 m contour on Fig. 3, enters the 38.5–42.5-min travel-time zone at only one location: the Ugamak Slide.

3. Landslide Motion

The far-field run-ups of 1 April 1946 lead us to suspect that the Ugamak Slide traveled at a substantial fraction of celerity. If the slide truly was the source of the tsunami, however, it must not have moved so fast that the waves back toward Unimak Island were suppressed. To consider whether these conflicting requirements could be satisfied simultaneously, we need to determine the speed of the slide for its entire motion.

Watts (1998) developed a wavemaker formalism for non-deforming underwater landslides, based on an approximate force-balance equation. His analytic solution for the displacement $s(t)$ of the center of mass of a landslide is

$$s(t) = s_0 \ln \left(\cosh \frac{t}{t_0} \right), \quad (1)$$

where s_0 and t_0 are the characteristic length and time of the motion, given by

$$s_0 = \frac{u_t^2}{a_0} \quad \text{and} \quad t_0 = \frac{u_t}{a_0}. \quad (2a,b)$$

Here a_0 and u_t are the initial acceleration and the terminal velocity of the landslide. The initial acceleration is

$$a_0 = g \frac{\gamma - 1}{\gamma + C_m} \sin \theta, \quad (3)$$

where γ is the specific density, θ is the slope angle, and C_m is an added mass coefficient (approximately unity). The terminal velocity is

$$u_t = \sqrt{gb} \sqrt{\frac{\pi(\gamma - 1)}{2C_d} \sin \theta}, \quad (4)$$

where b is the length of the slide and C_d is a drag coefficient (also taken as unity). From (1), we obtain the desired slide speed:

$$u(t) = \frac{ds(t)}{dt} = u_t \tanh \left(\frac{a_0 t}{u_t} \right). \quad (5)$$

The mean dip of the upper Aleutian forearc is 4.3° . Figure 4 shows bathymetric profiles down the axis of Ugamak Slide, interpolated from echo

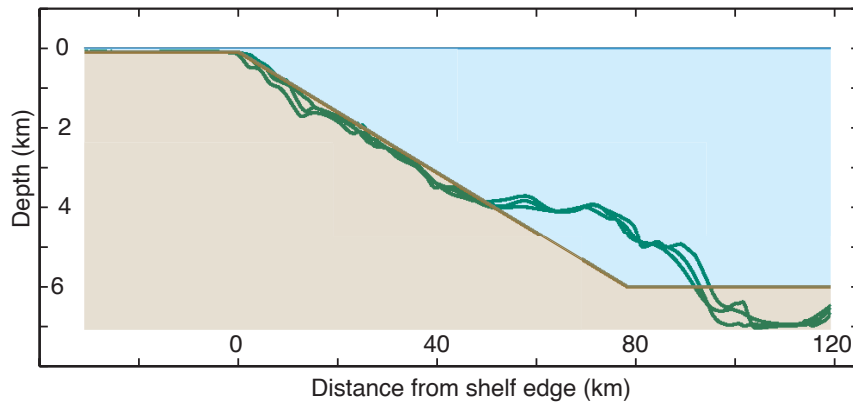


Figure 4: Profiles down the axis of the Ugamak Slide and our plane approximation to the slope.

soundings along sparse ship tracks (multibeam bathymetry does not yet exist for the Aleutian forearc west of 163°W). We assume the planar approximation shown, with a constant slope down to 6 km. While the actual slope descends to 7 km and crosses a terrace at 4 km, landslide motion is so controlled by the initial acceleration that such differences in deeper structure will not materially change our conclusions.

With a slope angle, θ , of 4.3° , an initial slide length, b_0 , of 40 km, and a specific density, γ , of 1.85, we obtain from (3) the starting acceleration, $a_0 = 0.22 \text{ m s}^{-2}$, and from (4) the terminal velocity, $u_t = 198 \text{ m s}^{-1}$. The characteristic time t_0 is defined in (2b). This time is the dominant period of the resulting tsunami (Watts, 2000). The value we obtain, 904 s, is indistinguishable from the tsunami period measured from tide gauge records.

4. A Deforming Landslide

In an actual landslide the toe will travel faster than the center of mass, while the head of the slide will travel more slowly. The slide will extend in length as it moves downslope (Fig. 5). Since the excitation of a tsunami will be most affected by the shallowest (and therefore the most slowly moving) part of the slide, simply solving for center of mass motion may not be enough to characterize tsunami generation.

Noting that in many experiments a deforming landslide lengthens linearly with time, Watts *et al.* (2000; 2001) proposed that the length b of a landslide should have the form

$$b(t) = b_0 [1 - \Gamma t (1 - e^{-Kt})]. \quad (6)$$

In laboratory experiments with granular material, the head of a landslide often hesitates before becoming fully involved in the downslope motion (e.g., Watts, 1997); the transient, e^{-Kt} , approximates this delay, provided $K \leq a_0/b_0\Gamma$. From the geometry of long-runout submarine landslides, Watts *et*

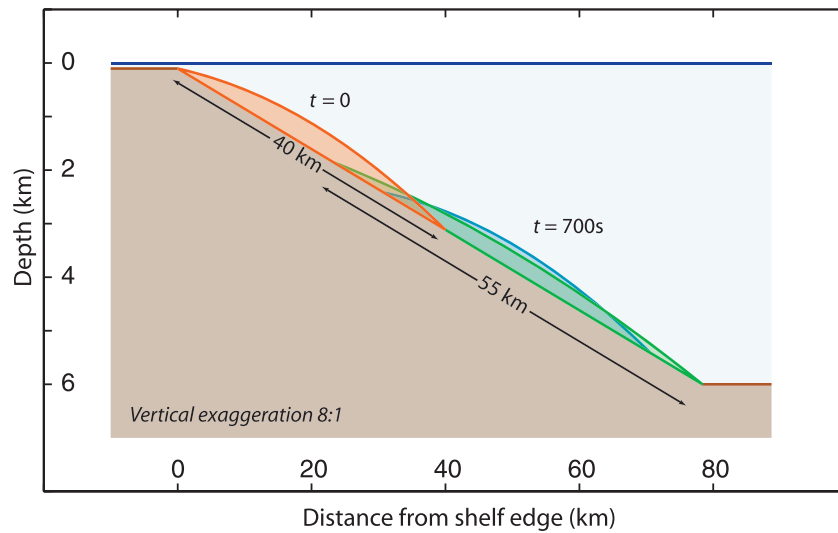


Figure 5: Sliding down the slope. The red-outlined body is the slide at the instant of failure. 700 s later the slide has moved to the blue outline if it has not deformed or to the green outline if it has deformed the maximum amount. In deforming the pre-slide length of 40 km expands to 55 km.

al. (2001) suggest that the maximum value of the lengthening factor is

$$\Gamma_{\max} \approx \frac{1}{6} \sqrt{\frac{g \sin \theta}{b_0}}. \quad (7)$$

5. Downslope Motion of the Ugamak Slide

Figure 6 shows how downslope displacement and velocity, from (1) and (2), vary with time, and how velocity as a fraction of local celerity varies with both time and depth (slide velocity as a fraction of local celerity is inaccurately referred to as “Froude number” in some papers). The functions displayed in Fig. 6 have been computed for the head (red), center of mass (green), and toe (blue) of the slide as well as for both a non-deforming landslide (solid lines) and for a maximally deforming landslide with $K = a_0/b_0\Gamma$ and $\Gamma = \Gamma_{\max}$ (dashed lines). Each curve ends at the trench axis.

The lower panels of Fig. 6 show that the head of the slide reaches 60% of celerity after about 200 s (by which time it has fallen from 105 m to 1000 m). The speed of the head of the slide remains above 60% of celerity for the remainder of the motion (i.e., until the slide runs into the trench). For deforming and non-deforming slides alike, the slide is above 60% of celerity for 700 continuous seconds. For all of that time, energy will be transferred from the slide to the water to be carried away in the advancing tsunami.

Even if the slide is non-deforming, its speed never exceeds 71% of celerity, so the suppression of landward waves (Tinti and Bertolucci, 2000) never occurs. Energy is therefore fed into both seaward and landward waves for the

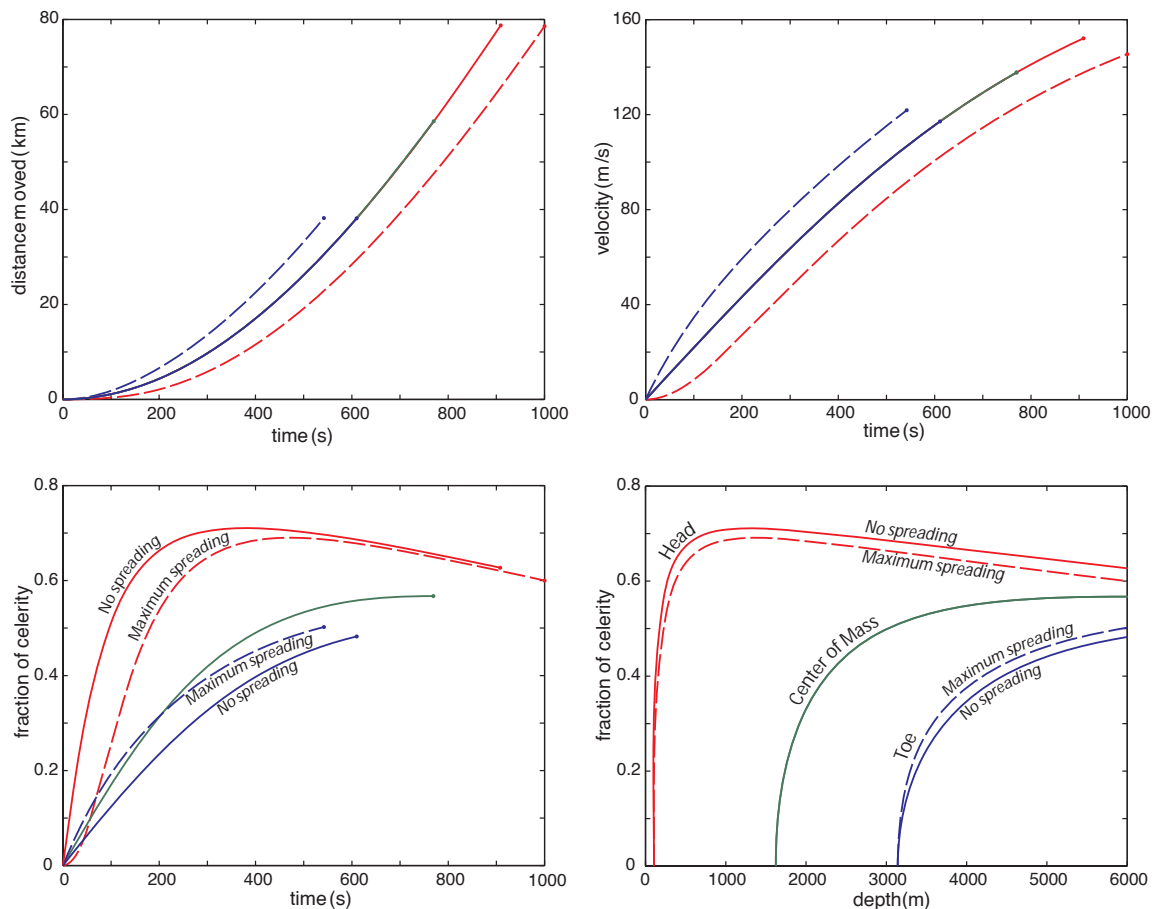


Figure 6: Evolution of the slide. Upper panels show distance and velocity of the slide versus time. Lower panels show the slide velocity as a fraction of celerity plotted as a function of time and of depth. In each panel red indicates the head of the slide, green the center of mass, and blue the toe. Solid curves are for a non-deforming slide, dashed curves for a deforming slide.

entire motion of the slide. At least qualitatively, destroying the lighthouse at Scotch Cap is not a problem.

To determine wave heights from the slide motion involves solution of the fluid dynamic equations. Because of the complex bottom shape, especially the shallow water over the shelf right at the head of the slide, anything short of a full 3-dimensional description of fluid flow is likely to be misleading. Nevertheless, with caution, much can be learned from approximate solutions. A rapid, approximate solution is provided by the code TOPICS, which, through curve fitting and appropriate scaling, uses the full fluid dynamic (though 2-D) modeling of Grilli and Watts (1999) to simulate tsunamis from submarine slope failures (the third dimension is approximated through a lateral spreading function). The output from TOPICS can be regarded as a snapshot of the ocean surface at time t_0 for waves generated over a smoothed and idealized structure. The TOPICS solution for the Ugamak Slide (computed assuming a slide thickness of 500 m, a length of 40 km, a width of 23 km, and a mean

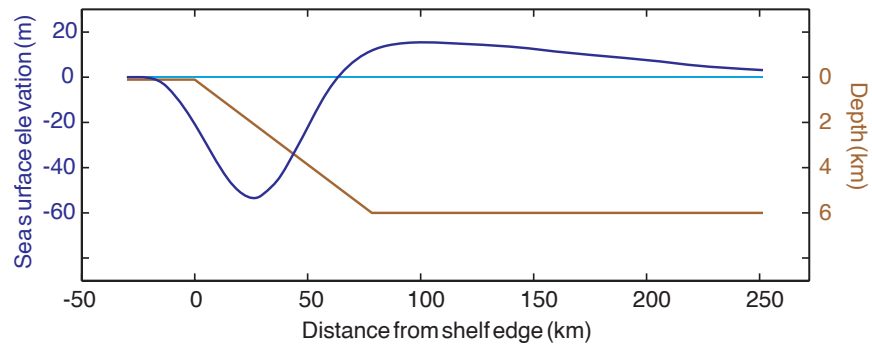


Figure 7: Sea-surface displacement computed by TOPICS.

depth before failure of 2 km) is shown in Fig. 7; this is a section along the axis of the slide, taken from the full two-dimensional solution.

Unfortunately, tsunami generation by the Ugamak Slide involves physics not modeled by Grilli and Watts (1999), water flow across the shelf, for example. The TOPICS output then loses its simple snapshot interpretation. Since the water-slide interaction has been correctly modeled, however, the surface profile of Fig. 7 shows the correct overall features. Figure 7 shows a trough amplitude of -54 m, centered over the middle of the pre-failure slide, and a peak amplitude of $+15$ m 20 km beyond the foot of the slope. The trough-to-peak distance is 66 km. Drawdown over the shelf edge is only approximate because of the incomplete physics, but it is clear that the amplitude of waves across the shelf must have been a significant fraction of the water depth.

6. Conclusions and Discussion

The case for a landslide source to the great tsunami of 1 April 1946 grows stronger. Unlike any earthquake source, the Ugamak Slide satisfies (qualitatively at least) the demands on the motion imposed by near-field and far-field wave heights. For most of its motion the slide traveled faster than 60% of celerity, coupling well enough with the water to project large waves across the Pacific. The perfect coupling at 100% celerity was never reached, however, so the landward waves were not suppressed. Scotch Cap Light was destroyed.

Travel times too support a slide-generated tsunami. The scar of Ugamak Slide occurs at exactly the location required for the slide to have been the source of the tsunami of 1946. While travel times do not eliminate an earthquake as a possible source, they do show that the best-fitting earthquake proposed so far is at least 35 km too far east.

Final proof of the landslide hypothesis will require high-resolution mapping, sampling, and dating of the Ugamak Slide, as well as numerical modeling to reproduce the Pacific-wide run-ups. We have already embarked on the modeling (Fryer and Watts, 2000).

The conditions that gave rise to the Ugamak Slide are unusual. A sys-

tem of rapidly prograding (and therefore poorly consolidated) glacial sediments deposited near sea level during glacial low stands was replaced by a sediment-starved system with retrogressive failure during the present high stand (Dobson *et al.*, 1996). The combination of poorly consolidated sediment, a gentle slope, a very shallow coastal shelf, and high seismicity, not only made a large-scale and long-duration landslide inevitable, it also guaranteed that the tsunami would be very large. The same conditions prevail along the Alaska Peninsula and the eastern Aleutian Islands as far west as Umnak Island, making this region potentially one of the most dangerous tsunami spawning grounds on Earth. There will be more events like 1946.

Acknowledgments. The travel-times of Fig. 3 were computed using the TTT package from *Geoware*. The sea-surface profile of Fig. 7 is a section through a 2-D prediction computed using the TOPICS model from *Applied Fluids Engineering, Inc.* SOEST Contribution No. 5709; HIGP Contribution No. 1161.

7. References

- Dobson, M.R., H.A. Karl, and T.L. Vallier (1996): Sedimentation along the fore-arc region of the Aleutian island arc, Alaska. In *Geology of the United States' Seafloor: The View from GLORIA*, edited by J.V. Gardner, M.E. Field, and D.C. Twichell, Cambridge University Press, Cambridge, 279–304.
- Fryer, G.J., and P. Watts (2000): The 1946 Unimak tsunami: near-source modeling confirms a landslide. *Eos Trans. AGU*, 81, F748.
- Fryer, G.J., P. Watts, and L.F. Pratson (2001): Source of the tsunami of 1 April 1946: A landslide in the upper Aleutian forearc. In *Prediction of Underwater Slide and Slump Hazards*, edited by P. Watts, C.E. Synolakis, and J.-P. Bardet, Balkema Publishers, Amsterdam, in press.
- Geist, E.L. (1998): Local tsunamis and earthquake source parameters. In *Advances in Geophysics*, 39, edited by R. Dmowska and B. Saltzman, Academic Press, San Diego, 117–209.
- Grilli, S.T., and P. Watts (1999): Modeling of waves generated by a moving submerged body: Applications to underwater landslides. *Eng. Analysis with Boundary Elements*, 23, 645–656.
- Heinrich, P., A. Piatanesi, H. Hébert, and E.A. Okal (2000): Near-field modeling of the July 17, 1998 event in Papua New Guinea. *Geophys. Res. Lett.*, 27, 3037–3040.
- Iida, K., D.C. Cox, and G. Pararas-Carayannis (1967): *Preliminary Catalog of Tsunamis Occurring in the Pacific Ocean*. Hawaii Inst. of Geophysics, Univ. of Hawaii, 274 pp.
- Johnson, J.M., and K. Satake (1997): Estimation of seismic moment and slip distribution of the April 1, 1946, Aleutian tsunami earthquake. *J. Geophys. Res.*, 102, 11,765–11,774.
- Karl, H.A., and P.R. Carlson (1996): Alaskan EEZ. In *Geology of the United States' Seafloor: The View from GLORIA*, edited by J.V. Gardner, M.E. Field, and D.C. Twichell, Cambridge University Press, Cambridge, 251–254.
- Lander, J.F. (1996): *Tsunamis Affecting Alaska 1737–1996*. Natl. Geophys. Data Center, Boulder, CO, 195 pp.
- Lander, J.F., and P.A. Lockridge (1989): *United States Tsunamis (Including United States Possessions) 1690–1988*. Natl. Geophys. Data Center, Boulder, CO, 265 pp.
- Pelayo, A.M. (1990): Earthquake source parameter inversion using body and surface

- waves: application to tsunami earthquakes and to Scotia Sea seismotectonics. Ph.D. thesis, Washington University, 252 pp.
- Pelayo, A.M., and D.A. Wiens (1992): Tsunami earthquakes; slow thrust-faulting events in the accretionary wedge. *J. Geophys. Res.*, *97*, 15,321–15,337.
- Sykes, L.R. (1971): Aftershock zones of great earthquakes, seismicity gaps, and earthquake prediction for Alaska and the Aleutians. *J. Geophys. Res.*, *76*, 8021–8041.
- Tinti, S., and E. Bortolucci (2000): Energy of water waves induced by submarine landslides. *Pure Appl. Geophys.*, *157*, 281–318.
- Watts, P. (1997): Water waves generated by underwater landslides. Ph.D. thesis, California Inst. of Tech., 319 pp.
- Watts, P. (1998): Wavemaker curves for tsunamis generated by underwater landslides. *J. Waterway Port Coast. Ocean Eng.*, *124*, 127–137.
- Watts, P. (2000): Tsunami features of solid block underwater landslides. *J. Waterway Port Coast. Ocean Eng.*, *126*, 144–152.
- Watts, P., S.T. Grilli, and C.E. Synolakis (2001): Tsunami generation by submarine mass failure I: Wavemaker models. *J. Waterway Port Coast. Ocean Eng.*, submitted.
- Watts, P., F. Imamura, and S.T. Grilli (2000): Comparing model simulations of three benchmark tsunami generation cases. *Sci. Tsunami Hazards*, *18*, 107–123.